Proceedings of the 4th International Conference on Functional Materials and Civil Engineering
DOI: 10.54254/2755-2721/2026.38018

Microfluidic Pre-processing Integrated Smart Lateral Flow Immunochromatographic Chip for Quantitative Analysis of Complex Samples

Shu Li

School of Chemistry, University of Glasgow, Glasgow, UK
oreolishu@163.com

Abstract. A microfluidic pre-processing integrated, smart lateral flow immunochromatographic chip is developed herein for quantitative analysis of complex samples. In this study, c-reactive protein (CRP) is chosen as the biomarker, while human whole blood serves as the matrix of interest. The proposed chip combines several functionalities, namely plasma separation, buffer mixing, lateral flow immunochromatographic detection, and smartphone readout, all in one process chain. The design is carried out with the aid of AutoCAD 2024 software, simulation performed by COMSOL Multiphysics 6.1, fabrication by means of PDMS soft lithography, and data analysis by using Python 3.11 equipped with OpenCV. CRP standards (0, 1, 5, 10, 25, and 50 mg/L) spiked in human whole blood with an appropriate anti-coagulant were used to establish the performance characteristics of the chip. Moreover, anonymous human serum was used for comparison against enzyme-linked immunosorbent assay (ELISA). The findings show that the mean flow time and plasma separation efficiency values are 168.4 ± 14.7 s and 87.6 ± 4.3%, respectively. The chip showed a detection range of 1-50 mg/L with R^2 = 0.986 and the limit of detection value was found to be 0.72 mg/L. The repeatability was acceptable as indicated by a variation coefficient less than 8% both intra- and inter-batches. Moreover, results showed excellent agreement between ELISA and the proposed chip (r = 0.963).

Keywords: microfluidic pre-processing, lateral flow immunochromatographic chip, smart detection, complex samples, C-reactive protein

1. Introduction

The utilization of lateral flow immunochromatographic assays (LFICAs) is common in rapid tests owing to its convenience and ability to be read using the naked eye. Challenges faced in quantifying the test-line include contamination from red blood cells (RBCs), inconsistency in viscosity, background coloring, and irregular migration pattern [1]. Thus, there has been substantial effort in recent years toward increasing accuracy by optimizing labeling strategy, controlling fluidic architecture, developing quantitative readouts, and improving digital signal processing in LFICA

© 2026 The Authors. This is an open access article distributed under the terms of the Creative Commons Attribution License 4.0 (https://creativecommons.org/licenses/by/4.0/).

DOI: 10.54254/2755-2721/2026.38018

[1]. Microfluidic devices represent an emerging solution to complicated sample manipulation that enables separation, metering, mixing, and transferring of fluids [2].

A good biomarker should be able to demonstrate the integrated functionality of such chips. C-reactive protein (CRP) is one example of an inflammation-related protein biomarker and can be employed to examine point-of-care assay efficacy. In the last few decades, advances in CRP assays have included microfluidic biosensors, electrochemical modules combined with a smartphone, and lateral flow immunoassay sensors [3-5]. Despite advancements, many techniques continue to require off-chip processed samples such as serum or plasma in order to obtain results. Practical applications for point-of-care assays demand that the device process whole blood directly, reduce interference from RBCs, produce a consistent signal intensity, and quantify analytes independent of other equipment.

In this work, a microfluidic pre-processed smart lateral flow immunochromatographic chip for CRP detection is designed. This chip incorporates four components; namely, plasma separation unit, mixing chamber, LF strip, and image-reader via smartphone. Validation tests use spiked whole blood samples and blinded serum samples for assessment in terms of flow, plasma separation efficiency, linearity, repeatability, limit of detection, and correlation coefficient compared to ELISA. The main aim of this experiment is to verify if microfluidic pre-processing with smartphone reading improves quantification of lateral flow immunochromatography.

2. Literature review

2.1. Microfluidic sample pre-processing

Microfluidic sample pre-processing consists of sample separation, filtration, dilution, mixing and controlled transfer prior to detection. In whole-blood test, the most critical task is the plasma separation because cell component will block the micro channels, change the path of capillary movement, also cause some effect on signal of optical detection of lateral-flow membrane. Passively do micro fluid separation when we have some things like this as diagnostic chips; there's no external pump driving us around based in capillary action forces inside a structure which also include hydrodynamics resistances within our system as well along with just the surface itself. Recently about paper-based and polymer-based microfluidics, low handling volume, low cost and portability of device are crucial points for point-of-care testing [6]

2.2. Lateral flow immunochromatographic detection

Lateral flow immunochromatographic detection relies on recognizing antigens with antibodies on a nitrocellulose membrane. As to CRP detection, gold nanoparticle-tagged anti-CRP antibodies function as signposts for us to read; CRP antibody conjugate binds to our test line so that we could tell if it passed all right along our way. Recently there were improved CRP LFD's which use enhanced labels, electrochemiluminescent signals, and better full-range detection setups to be able to quantify [7]. But traditional ones are still affected by background interference and changeable lines caused by lacking enough samples to be prepared. When the complicated samples were involved, T/C rate proved to be quite constant in comparison to initial raw intensity value of test lines, due mainly to some partial correction offered both for strip-related variation and also the fluctuations regarding flows.

DOI: 10.54254/2755-2721/2026.38018

2.3. Smart quantitative readout

Smart quantitative readout transforms visible immunochromatographic signals into numerical outputs through standardized imaging and computational signal extraction. Smartphone cameras are increasingly used as portable readers because they can acquire high-resolution images without additional laboratory instruments [8]. When combined with a fixed imaging box, stable LED illumination, and image-processing algorithms, smartphone readout can reduce subjective visual interpretation and improve weak-signal recognition. Recent algorithmic studies also show that region-of-interest localization, grayscale conversion, background correction, and multi-line signal extraction can improve the reproducibility of lateral flow quantification [9, 10]. Therefore, smart readout is essential for transforming visual lateral flow results into semi-quantitative or quantitative biomarker values.

3. Experimental methods

3.1. Chip design and fabrication

Chip architecture was designed using AutoCAD 2024. Dimensions of the device include length of 75 mm, width of 25 mm, and thickness of 5 mm. Microfluidics consist of sample inlet (20 μL), plasma separator, 15 μL buffer mixture chamber, and outlet that is linked to lateral flow strip. Dimensional layout of the microchannel is width = 300 μm and depth = 80 μm. This arrangement was selected to ensure sufficient capillary force to induce fluid movement while avoiding unnecessary pressure loss and minimizing cellular intrusion into the detection zone. Laminar flow and pressure profile simulation with COMSOL Multiphysics 6.1 was performed at a flow rate of 2 μL/min.

Manufacturing of the chip was done by PDMS soft lithography technique. First, SU-8 mold for the microchip was created on the silicon wafer according to the AutoCAD design. In order to create PDMS mold, prepolymer and curing agent were mixed at the ratio of 10:1; afterwards, it was degassed, poured, and baked at 80°C for 60 min. After demolding process, inlet and outlet holes were punched. Glass surface and PDMS were then plasma treated and bonded to form sealed microchannel structures. The lateral flow strip was attached to the downstream chamber. Test line was coated with anti-CRP capture antibody, whereas control line with goat anti-mouse IgG. Lateral flow strips contained four layers: sample pad, conjugate pad, nitrocellulose membrane, and absorbent pad.

3.2. Reagents, samples, and data setting

Concentrations of 0, 1, 5, 10, 25, and 50 mg/L of CRP standard solutions were used to cover the range from non-inflammatory to high inflammatory concentrations. Each concentration was analyzed in quintuplicates on human anticoagulated whole blood. This gave 120 samples per standard concentration and 600 samples overall, covering blank, low, moderate, and high concentrations. Thirty human anonymized serum samples were assayed by chip and ELISA. Serum values were used only for comparison of methods.

CRP gold nanoparticles with a diameter of 40 nm were conjugated to anti-CRP monoclonal antibody. The conjugate was incubated in 1% bovine serum albumin dissolved in PBS buffer with pH = 7.4. Running buffer included PBS with 0.05% Tween-20 and 1% bovine serum albumin. Data recorded for each experiment included sample name, CRP concentration, batch number, replicate

DOI: 10.54254/2755-2721/2026.38018

number, flow time, plasma separation rate, intensity of the test line, intensity of the control line, intensity of the background, corrected intensity of the test line, corrected intensity of the control line, and T/C ratio. All image files, concentration data, and signal extraction output data were saved in folders compatible with CSV format.

3.3. Image processing and statistical analysis

Images of chips were generated by capturing with iPhone 14 that was placed inside a closed LED imaging chamber. The fixed distance between the smartphone and the chip was set at 12 cm. All the images were taken 15 minutes after sample addition under the same camera mode, exposure, resolution, and illumination conditions. Image post-processing was carried out using Python 3.11 and OpenCV. In the process, the program cropped the detection area, converted RGB images into grayscale, detected the locations of test and control line areas, measured the intensity of local backgrounds, and obtained T/C ratios as the corrected output.

All statistical calculations were performed in SPSS version 29. Linear regression was used to analyze the correlations between the concentrations of CRP and the T/C ratios. The limit of detection was calculated as mean background intensity plus 3 standard deviations. The repeatability was analyzed using the coefficient of variations in replicates and among blood batches. Correlation and comparison between chip detection results and those from ELISA analysis were performed using Pearson's correlation and Bland-Altman methods.

4. Experimental process

4.1. Chip preparation and pre-test check

Prior to initiating the test, all chips were kept at ambient temperature for 20 minutes. Microchannels, inlet port, buffer tank, bonding zone, and lateral flow strips were inspected under the stereo microscope. Chips having blocked channels, leakage problems, inadequate bonding, damaged membranes, or no control line response were discarded from any further experiment. For each batch of chips fabricated, three chips were used to perform running buffer to ensure background consistency. The illumination of the LED light source was done five minutes prior to imaging. Image of blank chips was utilized in the OpenCV script to identify the background region.

The corrected T/C signal was calculated as shown in Equation (1):

$$R_{TC} = \frac{I_{B,T} - I_T}{I_{B,C} - I_C + \delta} \tag{1}$$

where R_{TC} is the corrected T/C ratio, I_T is the grayscale intensity of the test-line region, I_C is the grayscale intensity of the control-line region, $I_{B,T}$ is the local background intensity near the test line, $I_{B,C}$ is the local background intensity near the control line, and δ is a very small constant used to avoid division by zero. This formula is correct for colorimetric lateral flow images because darker lines have lower grayscale intensity; subtracting line intensity from local background converts color development into a positive signal.

DOI: 10.54254/2755-2721/2026.38018

4.2. Whole-blood loading and on-chip pre-processing

In each test, 20 μL of whole blood was injected into the sample inlet using a calibrated micropipette. With the help of capillary force, the sample got transported inside the separation channel. The erythrocytes stayed in the upstream area, while the plasma flowed towards the buffer chamber. The time of flow from the start of sample injection until the appearance of liquid out of the outlet was measured. After the plasma entered the buffer chamber, 40 μL of buffer was added through the buffer inlet, creating a mixture. This mixture was then transported across the nitrocellulose membrane by the lateral flow strip, which resulted in the rehydration of the gold nanoparticle conjugate.

Plasma separation efficiency was calculated as shown in Equation (2):

$$E_p = (1 - \frac{H_{out}}{H_{in}}) \times \frac{V_p}{V_b} \times 100 \quad (2)$$

where E_p is plasma separation efficiency, H_{in} is the initial hematocrit-related cell fraction before separation, H_{out} is the residual cell fraction in the plasma outlet, V_p is the plasma volume entering the buffer chamber, and V_b is the loaded whole-blood volume. This formula is appropriate because it jointly evaluates cellular removal and usable plasma transfer, rather than reporting only visual separation.

4.3. Signal acquisition and data output

Each chip was inserted into the LED imaging chamber after 15 minutes, and then images were taken using an iPhone 14. The images obtained were coded based on the type, concentration level, batch, and replicate number. The images were uploaded in the Python image processing folder where they were further analyzed by running an OpenCV script to process the images in batch mode. The output of the analysis contained the intensity of the test-line, intensity of the control-line, background reading, adjusted test-line reading, adjusted control-line reading, and the T/C ratio. Those records without a clear control-line were disregarded. The remaining records were further analyzed using SPSS Statistics 29.

5. Experimental results

5.1. Microfluidic pre-processing performance

The integrated chip showed stable capillary-driven flow and effective whole-blood pre-processing. The mean flow time from sample loading to outlet appearance was 168.4±14.7 s, and plasma separation efficiency reached 87.6±4.3% (see Table 1). The residual cell interference index remained below 0.10, indicating that most cellular components were retained before the detection region. Blank-chip background fluctuation was low, supporting reliable image-based signal correction.

Table 1. Microfluidic pre-processing and quantitative detection performance

Indicator	Result
Flow time from inlet to outlet	168.4±14.7 s

DOI: 10.54254/2755-2721/2026.38018

Table 1. (continued)

Plasma separation efficiency	87.6±4.3%
Residual cell interference index	0.083±0.021
Blank T/C ratio	0.041±0.009
Limit of detection	0.72±0.11 mg/L
Linear range	1–50 mg/L
Calibration equation	$R_{TC} = 0.031 + 0.018C_{CRP}$
Linearity	$R^2 = 0.986 \pm 0.006^{**}$
Mean intra-batch CV	5.84±1.26%
Mean inter-batch CV	7.92±1.54%

Note: **p<0.01 for calibration linearity.

5.2. Quantitative detection and repeatability

The corrected T/C ratio increased consistently with CRP concentration. Mean T/C values were 0.041±0.009, 0.052±0.011, 0.118±0.018, 0.213±0.026, 0.482±0.041, and 0.934±0.066 at 0, 1, 5, 10, 25, and 50 mg/L, respectively. The coefficient of variation remained within an acceptable range for both intra-batch and inter-batch testing. Slightly larger variation occurred at 50 mg/L because the test-line signal approached optical saturation (see Figure 1). The corrected T/C ratio showed better quantitative stability than raw test-line intensity because it reduced background and control-line variation.

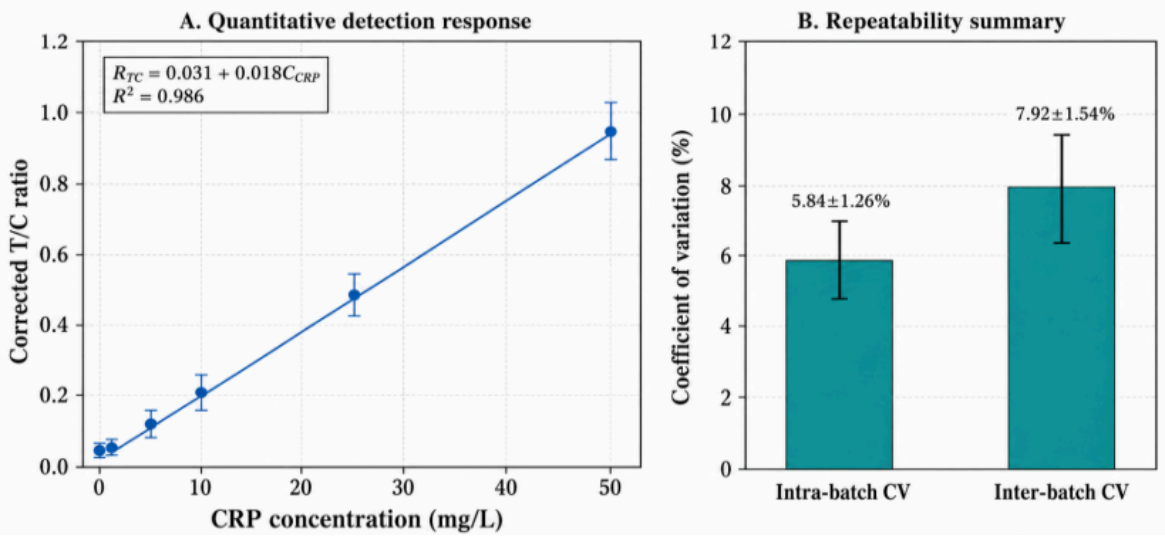

Figure 1. Quantitative detection and repeatability of the microfluidic LFIA chip

DOI: 10.54254/2755-2721/2026.38018

5.3. Complex sample testing and ELISA agreement

The 30 anonymous serum samples showed strong agreement between the proposed chip and ELISA. Pearson correlation reached r=0.963±0.018**, and Bland-Altman analysis showed a mean bias of -0.38±1.46 mg/L (see Table 2). Most differences remained within the 95% agreement interval. These results indicate that the chip can generate quantitative values close to ELISA while retaining the operational advantages of microfluidic pre-processing and smartphone readout.

Table 2. CRP detection response and ELISA agreement

Test condition	Chip result / agreement indicator
0 mg/L CRP	0.041±0.009
1 mg/L CRP	0.052±0.011
5 mg/L CRP	0.118±0.018
10 mg/L CRP	0.213±0.026
25 mg/L CRP	0.482±0.041
50 mg/L CRP	0.934±0.066
Pearson correlation with ELISA	r=0.963±0.018*
Mean bias versus ELISA	-0.38±1.46 mg/L
95% agreement interval	-3.24 to 2.48 mg/L
Invalid control-line rate	1.67±0.58%

Note: **p<0.01 compared with the null correlation.

6. Conclusion

This study demonstrates a microfluidic pre-processing integrated smart lateral flow immunochromatographic chip for quantitative CRP analysis in complex samples. The device integrates whole-blood plasma separation, buffer mixing, lateral flow immunodetection, and smartphone-based image analysis. Experimental results show stable flow control, high plasma separation efficiency, low residual cell interference, strong calibration linearity, acceptable repeatability, and close agreement with ELISA. The corrected T/C ratio provides a practical signal for reducing background and strip-variation effects. The proposed chip offers a feasible route for point-of-care CRP measurement from whole blood and can be extended to other biomarkers after antibody replacement and calibration redesign. Future work should improve long-term storage stability, expand clinical sample validation, and integrate automated smartphone applications for direct concentration output.

References

[1] Dey, M. K., Iftesum, M., Devireddy, R., & Gartia, M. R. (2023). New technologies and reagents in lateral flow assay (LFA) designs for enhancing accuracy and sensitivity. *Analytical Methods, 15*, 4351–4376.

[2] Wang, Y., Nunna, B. B., Talukder, N., Etienne, E. E., & Lee, E. S. (2021). Blood plasma self-separation technologies during the self-driven flow in microfluidic platforms. *Bioengineering, 8*(7), 94.

[3] Tavakolidakhrabadi, A., Stark, M., Küenzi, A., Carrara, S., & Bessire, C. (2025). Optimized microfluidic biosensor for sensitive C-reactive protein detection. *Biosensors, 15*(4), 214.

DOI: 10.54254/2755-2721/2026.38018

[4] Boonkaew, S., Szot-Karpińska, K., Niedziółka-Jönsson, J., de Marco, A., & Jönsson-Niedziółka, M. (2024). NFC smartphone-based electrochemical microfluidic device integrated with nanobody recognition for C-reactive protein. *ACS Sensors, 9*(6), 3066–3074.
[5] Park, J. (2022). Lateral flow immunoassay reader technologies for quantitative point-of-care testing. *Sensors, 22*(19), 7398.
[6] Aryal, P., & Henry, C. S. (2024). Advancements and challenges in microfluidic paper-based analytical devices: Design, manufacturing, sustainability, and field applications. *Frontiers in Lab on a Chip Technologies, 3*, 1467423.
[7] Hong, D., Kim, K., Jo, E. J., & Kim, M. G. (2021). Electrochemiluminescence-incorporated lateral flow immunosensors using $Ru(bpy)_3^{2+}$-labeled gold nanoparticles for the full-range detection of physiological C-reactive protein levels. *Analytical Chemistry, 93*(22), 7925–7932.
[8] Colombo, M., Bezinge, L., Rocha Tapia, A., Shih, C.-J., deMello, A. J., & Richards, D. A. (2023). Real-time, smartphone-based processing of lateral flow immunoassays. *Sensors & Diagnostics, 2*, 100–110.
[9] Chen, S.-J., Lu, S.-Y., Tseng, C.-C., Huang, K.-H., Chen, T.-L., & Fu, L.-M. (2024). Rapid microfluidic immuno-biosensor detection system for the point-of-care determination of high-sensitivity urinary C-reactive protein. *Biosensors, 14*(6), 283.
[10] Zhang, S., Guo, J., Wang, Z., Li, X., & Liu, Y. (2023). A quantitative detection algorithm for multi-test line lateral flow immunoassay based on smartphone image processing. *Sensors, 23*(14), 6401.